

See discussions, stats, and author profiles for this publication at: <https://www.researchgate.net/publication/234908145>

Thermal and mass diffusion in a semidilute good solvent-polymer solution

ARTICLE *in* THE JOURNAL OF CHEMICAL PHYSICS · JULY 1999

Impact Factor: 2.95 · DOI: 10.1063/1.479498

CITATIONS

86

READS

10

5 AUTHORS, INCLUDING:



Matthew Briggs

Los Alamos National Laboratory

40 PUBLICATIONS 803 CITATIONS

SEE PROFILE



Robert W. Gammon

University of Maryland, College Park

64 PUBLICATIONS 1,834 CITATIONS

SEE PROFILE



J. F. Douglas

National Institute of Standards and Technolo...

428 PUBLICATIONS 14,795 CITATIONS

SEE PROFILE

Thermal and mass diffusion in a semidilute good solvent-polymer solution

K. J. Zhang, M. E. Briggs, R. W. Gammon, J. V. Sengers, and J. F. Douglas

Citation: *The Journal of Chemical Physics* **111**, 2270 (1999); doi: 10.1063/1.479498

View online: <http://dx.doi.org/10.1063/1.479498>

View Table of Contents: <http://scitation.aip.org/content/aip/journal/jcp/111/5?ver=pdfcov>

Published by the [AIP Publishing](#)

Articles you may be interested in


[Critical assessment of diffusion coefficients in semidilute to concentrated solutions of polystyrene in toluene](#)
J. Chem. Phys. **130**, 124905 (2009); 10.1063/1.3098403

[Correlation between thermal diffusion and solvent self-diffusion in semidilute and concentrated polymer solutions](#)
J. Chem. Phys. **126**, 214901 (2007); 10.1063/1.2738467

[Thermal diffusion of dilute polymer solutions: The role of solvent viscosity](#)
J. Chem. Phys. **125**, 214904 (2006); 10.1063/1.2393230




[Collective and thermal diffusion in dilute, semidilute, and concentrated solutions of polystyrene in toluene](#)
J. Chem. Phys. **119**, 11977 (2003); 10.1063/1.1623745

[Influence of intermolecular interaction on the dynamics of good solvent-polymer solutions](#)
J. Chem. Phys. **115**, 1943 (2001); 10.1063/1.1383054



AIP | The Journal of
Chemical Physics

Meet The New Deputy Editors

	Peter Hamm		David E. Manolopoulos		James L. Skinner
---	-------------------	---	------------------------------	---	-------------------------

Thermal and mass diffusion in a semidilute good solvent-polymer solution

K. J. Zhang,^{a)} M. E. Briggs,^{b)} R. W. Gammon, and J. V. Sengers
*Institute for Physical Science and Technology, and Department of Chemical Engineering,
 University of Maryland, College Park, Maryland 20742*

J. F. Douglas

Polymers Division, Materials Science and Engineering Laboratory, NIST, Gaithersburg, Maryland 20899

(Received 5 February 1999; accepted 29 April 1999)

The Soret coefficient S_T and collective (mass) diffusion coefficient D_c of polystyrene dissolved in the good-solvent toluene has been measured over a range of concentrations and molecular masses with an optical beam-deflection method. Our measurements indicate that S_T scales inversely with the polymer translational diffusion coefficient in dilute solutions, exhibits a power-law scaling with polymer concentration, and an independence of polymer molecular mass in semidilute solutions. These findings are consistent with the known scaling of $1/D_c$ in dilute and semidilute polymer solutions, the relative insensitivity of the thermal-diffusion coefficient D_{th} of polystyrene in toluene to polymer concentration, and the relation $S_T = D_{th}/D_c$ from irreversible thermodynamics. We are able to represent our S_T and D_c data by theoretically motivated reduced-concentration master curves, but the concentration-molecular mass scaling variables are found to be different for each transport property, a result contrary to theoretical expectations. However, the asymptotic concentration scaling exponents deduced from these data fits are compatible with de Gennes' scaling arguments for D_c and with modern estimates of the chain-size exponent ν for swollen polymers in good solvents. © 1999 American Institute of Physics. [S0021-9606(99)51128-8]

I. INTRODUCTION

The thermodynamic and transport properties of polymer solutions have been studied intensively in the last two decades by applying scaling concepts and renormalization-group theory.¹⁻³ It is conventional to classify polymer solutions into dilute, semidilute, and concentrated solution regimes because of property regularities which arise in these concentration ranges. Scaling and renormalization-group theory are applicable to the dilute and semidilute regimes where polymer concentration fluctuations are appreciable, while lattice mean-field theory becomes applicable at high polymer concentrations where concentration fluctuations are small and chain-packing effects become important. The theory of the equilibrium properties of polymer solutions is well developed and supported by many experiments,¹⁻³ but the theoretical understanding and experimental investigation of the transport properties of polymer solutions is much less complete.

One of the most extensively studied and basic transport properties is the collective diffusion coefficient D_c ,⁴⁻⁸ which describes the rate at which polymer-concentration fluctuations decay. In dilute polymer solutions D_c can be expressed through the infinite-dilution Stokes-Einstein relation for single-particle motion $D_{c0} = k_B T / (6\pi\eta_s R_H)$ and a virial expansion in concentration:

$$D_c = D_{c0} [1 + k_D c + O(c^2)], \quad (1)$$

where k_B is Boltzmann's constant, T the temperature, η_s the viscosity of the solvent, R_H the hydrodynamic radius of the polymer, k_D the leading virial coefficient of D_c , and c the concentration of polymer in g cm^{-3} . D_c and k_D reflect both the thermodynamic and hydrodynamic interparticle interactions.^{3,8} A linear concentration dependence has been observed experimentally for dilute polymer solutions in good solvents where interchain interactions are strong ($k_D > 0$), as well as in theta solvents where the osmotic second virial coefficient vanishes and hydrodynamic interactions predominate^{5,6} ($k_D < 0$).

The order of magnitude of the onset of the semidilute regime of polymer solutions is commonly estimated by a geometrical "overlap concentration" c^* :

$$c^* = \frac{M_w}{\frac{4\pi}{3} N_A R_g^3}, \quad (2)$$

where M_w is the mass-average molecular mass,⁹ N_A is Avogadro's number, and R_g the radius of gyration of the flexible polymer coil. Alternatively, c^* may be defined as the reciprocal of the intrinsic viscosity $[\eta]$, the leading virial coefficient for the viscosity of the polymer solution. Interchain interactions become appreciable when $c/c^* \sim O(1)$, so that leading-order virial expansions, such as Eq. (1), tend to exhibit deviations from linearity near this concentration.

Experimental observations indicate that D_c becomes independent of the molecular mass in semidilute and concentrated solutions and a scaling with polymer concentration is often observed. De Gennes and co-workers¹⁰ have invoked

^{a)}Present address: Electronic Data Systems, Human Resources Group, 13600 EDS Drive, Herndon, VA 20171.

^{b)}Present address: Physics Department, University of Utah, Salt Lake City, UT 84112.

scaling arguments to predict the exponent describing the concentration dependence of D_c in the semidilute regime:

$$D_c \sim (c/c^*)^{x_D}, \quad x_D = \nu/(3\nu - 1), \quad c/c^* \geq O(1). \quad (3)$$

This leads to an exponent $x_D = 0.75$ when the chain-size exponent ν describing the mass scaling of R_g is taken to have the simple Flory^{1,3} estimate, $\nu = 3/5$. More refined estimates² of ν obtained from renormalization-group, lattice-enumeration, and Borel-resummation methods are close to $\nu \approx 10/17 \approx 0.588$, corresponding to the more precise scaling-model estimate $x_D = 10/13 \approx 0.77$. Several experimental measurements in the semidilute regime, however, have yielded an exponent x_D around 0.65, smaller than the value predicted^{11–13} by the scaling theory. Brown and Nicolai⁷ suggested that the exponent x_D should become larger for much of the existing data once corrections for “backflow” (counter-motion in the solvent induced by the motion of polymer segments) are applied to the collective diffusion-coefficient data. Geissler and Hecht¹⁴ have introduced a separate correction involving the change in the translational diffusion coefficient of the solvent in the presence of polymer which leads to an increase in the exponent x_D to a value closer to the theoretical value in Eq. (3). Lodge¹⁵ has recently reviewed the phenomenology of the modification of the solvent dynamics arising from the presence of polymers in solution and has emphasized the importance of the coupling between the solvent and polymer dynamics in properly deducing the concentration dependence of the transport properties of polymer solutions. It is our view that the theoretical foundations of these corrections need further examination and these corrections are avoided in the present paper.

Studies of thermal diffusion in polymer solutions have been relatively few and only a small number of measurements on the Soret coefficient S_T have been reported. Meyerhoff and Nachtigall¹⁶ measured the thermal-diffusion coefficient $D_{th} = S_T D_c$ of polystyrene solutions in toluene with an optical diffusion cell, and the concentration differences of the samples were determined by observing the Guoy fringe pattern caused by interference of light passing through the liquid. Their experiments indicated that there is a pronounced molecular-mass dependence of S_T and D_c in the dilute concentration regime and a tendency for S_T to become independent of molecular mass in semidilute polymer solutions. The thermal-diffusion coefficient D_{th} was found to be roughly independent of molecular mass and of concentration for the ranges investigated.

Ecenarro *et al.*¹⁷ revisited the problem of thermal-diffusion measurements of polystyrene in toluene using a thermogravitational column. Their experiments show a slight decrease of the thermal-diffusion coefficient in the dilute regime with increasing concentration. Köhler *et al.*¹⁸ recently also measured S_T and D_c of polystyrene solutions in toluene in the dilute regime using a forced Rayleigh-scattering method. Their measurements are more accurate compared to the previous experiments for polystyrene–toluene solutions. They also confirm that D_{th} is relatively independent of concentration.

In the 1970's Giddings *et al.*^{19,20} developed a thermal-field flow-fractionation method and measured the thermal-

diffusion factor $\alpha_T = T S_T$ of dilute solutions of polystyrene in eight different solvents. The general dependencies of the thermal-diffusion factor α_T on temperature and molecular mass are similar for all the eight solvents. Their results support the conclusion that D_{th} is independent of the molecular mass in the dilute regime. This independence of the thermal-diffusion coefficient on the molecular mass was later rationalized by Brochard and de Gennes²¹ as due to the absence of long-range coupling between monomers undergoing thermal diffusion. In a later work, Giddings *et al.*²⁰ studied α_T for dilute solutions of polystyrenes of different branched-chain architectures (linear, star, or comblike) and found that D_{th} is independent of the chain topology.

The thermal-diffusion experiments mentioned above are mainly concerned with dilute solutions. We have investigated thermal diffusion in solutions of polystyrene in toluene with an optical beam-deflection method and have measured S_T and D_c of solutions of seven different molecular masses over a concentration range from dilute to semidilute. Power-law exponents describing the concentration and molecular mass dependencies of S_T and D_c have been determined and S_T and D_c have both been fitted to a common master curve by using judicious choices of the reducing concentration variables.

In Sec. II we briefly discuss the experimental arrangement, sample preparation, and procedure of data interpretation. Section III presents the measurements of the concentration derivative of the refractive index $(dn/dw)_{T,p}$ and the determination of the temperature derivative of the refractive index $(dn/dT)_{w,p}$ which is needed to interpret the optical beam-deflection signal. Experimental results for S_T , D_c , and D_{th} are summarized in Sec. IV and a reduction of these data to a master curve describing the concentration and molecular-mass dependence of these properties is given in Sec. V.

II. EXPERIMENTAL ARRANGEMENT AND WORKING EQUATIONS

A. Apparatus

The optical beam-deflection method was first applied by Giglio and Vendramini^{22,23} to polymer solutions and molecular binary liquid mixtures close to a critical mixing point. The method was subsequently improved and used by Kolodner *et al.*²⁴ for ethanol–water mixtures. We have developed an optical beam-deflection apparatus²⁵ that differs substantially from those used by Giglio and Vendramini and by Kolodner *et al.* The optical cell of our apparatus utilizes a different temperature-control mechanism, a long sample path length, a controlled uniform temperature profile along the liquid layer, and a shorter transient time for establishing a temperature gradient. These features yield a lower uncertainty of the S_T measurements and allow for a simultaneous measurement of D_c . This optical beam-deflection apparatus has been successfully used for measuring S_T and D_c in normal liquid mixtures,²⁵ for which S_T is typically two orders smaller than for polymer solutions.

Figure 1 shows a schematic representation of the optical beam-deflection experiment. Initially the polystyrene-

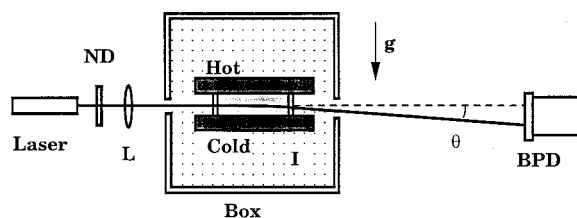


FIG. 1. Schematic diagram of the experimental arrangement. Laser: He–Ne laser. NDF: neutral density filter. L: focal lens. Hot and cold: top and bottom plates of the cell. I: insulation material. Box: thermostated copper box. BPD: beam-position detector.

solution sample, confined between the top and bottom plates, is in a thermal equilibrium state with the two plates having the same temperature and a laser beam passes through the liquid horizontally. A temperature gradient is then imposed onto the polymer solution by changing the temperature of the top plate to a higher value. A temperature gradient and a concentration gradient will build up in the liquid layer following thermal conduction and thermal diffusion, which induce a refractive-index gradient and bending of the laser beam. The collective mass-diffusion coefficient D_c can be deduced from the rate of change of the beam deflection and the Soret coefficient S_T is determined from the final beam deflection. A more detailed description of the experimental apparatus and of the sample cell can be found in a previous publication.²⁵

To interpret the beam-deflection signal we also measured the refractive index of the polymer solutions with an Abbé refractometer. The principle of the operation of the Abbé refractometer is discussed in Ref. 26. The refractive index of a liquid is found by measuring the critical angle of the total reflection of a light beam transmitted through the liquid. We used white light taking its wavelength as equal to the wavelength of sodium light, 5893 Å, for which the Abbé refractometer was calibrated. Our calibration measurements with white light and with sodium light indicate that the difference in the measured refractive indices corresponding to the two sources is smaller than the reading uncertainty of the refractometer and can be neglected. By using the dispersion table associated with the refractometer, the refractive index measured with the white light is then transformed into a value for the refractive index for light with wavelength λ

$=6328 \text{ Å}$ corresponding to the He–Ne laser used in the optical beam-deflection measurements. In our measurements the temperature of the Abbé refractometer was controlled at $T=(25.00 \pm 0.05)^\circ\text{C}$ with water from a Forma circulating bath. The standard uncertainty of the measured refractive index for the polymer solutions is $\pm 2 \times 10^{-4}$, limited by the resolution of the refractometer.

B. Samples

The linear polystyrene samples of various molecular masses⁹ were purchased from the Tosoh Corporation.²⁷ The characteristics of the samples are given in Table I with the first four columns of the data from the specifications provided by the manufacturer, the overlap concentration c^* calculated from Eq. (2), and the last column from a commercial test to be discussed below. In our experiments, we employed samples of seven different molecular masses ranging from 2.6×10^3 to $3.8 \times 10^6 \text{ g/mol}$, with the radius of gyration of the samples between 1.3 and 100 nm. All polymer samples were purchased as dry, white, solid material (powders or chunks) sealed in bottles.

The polydispersity of the samples reported by the manufacturer is narrow, with M_w/M_n from 1.01 to 1.05, as shown in Table I, where M_w is the mass-average molecular mass⁹ and M_n is the number-average molecular mass. The company provided the following description of their GPC analysis. For each sample, the molecular mass M_w and molecular mass distribution M_w/M_n were estimated at 25°C with a liquid chromatograph (HLC-802A) and a low-angle laser scattering photometer (LS-800) on a set of two to four serially connected polystyrene resin columns (TSK gel G6000, 4000, 2000 HXL, etc.). Tetrahydrofuran (THF) was used as mobile phase. The average molecular mass was computed from a calibration curve obtained by using a series of TSK standard polystyrene samples.

To obtain an independent polydispersity check we sent five of the seven samples to Polymer Source Inc., Quebec,²⁸ for a GPC commercial test. The company made elution chromatography at 30°C with a Varian Liquid Chromatograph (Varian 9002) equipped with a refractive-index detector (Varian RI-4) and an UV detector (Varian 9050). Measurements were made on three resin columns (TSK gel G6000, 4000, 2000 HXL) calibrated with monodisperse standards of

TABLE I. Characteristics of the polystyrene samples.

Type	M_w^a (g mol^{-1})	M_w/M_n^b (Manufacturer)	$[\eta]^c$ ($\text{cm}^3 \text{g}^{-1}$)	c^{*d} (g cm^{-3})	M_w/M_n^e (Commercial test)
A-2500	2 630	1.05	0.041	0.463	1.12
F-1	9 100	1.02	0.080	0.175	1.04
F-4	37 900	1.01	0.171	0.0570	...
F-10	96 400	1.01	0.270	0.0274	1.02
F-20	190 000	1.04	0.359	0.0161	1.03
F-80	706 000	1.05	0.713	0.0057	...
F-380	3 840 000	1.04	1.59	0.0015	1.13

^a M_w is the weight-average molecule weight (Ref. 9).

^b M_n is the number-average molecular weight.

^c $[\eta]$ is the intrinsic viscosity and is taken from the specifications of the manufacturer, measured at 34.5°C .

^d c^* is the "overlap concentration" given by Eq. (2).

^ePolymer Sources, Inc. estimates the relative standard uncertainty of their molecular-weight ratios as $\pm 5\%$.

THF containing a mass fraction of 3% of dried triethylamine as eluent. The THF was distilled over sodium/benzophenone complex and filtered through a 0.5 μm pore, polytetrafluoroethylene membrane filter. Polymer Source Inc. suggested that their estimation of the polydispersity shown in Table I could have a relative standard uncertainty of $\pm 5\%$. Within this uncertainty, their analysis of sample polydispersity agrees with the manufacturer's values for the samples of intermediate molecular mass. For samples of the lowest and the highest molecular mass, the commercial test lies slightly outside the stated relative standard uncertainty, but we note that there was increased noise in the baseline of the commercial tests of these two samples.

The toluene solvent was Fisher certified reagent purchased from Baker Chemical Co. The purity of the toluene is better than 99.8% (GC assay by Baker) and was used without further purification.

Polymer solutions at a given concentration w (w = mass fraction) were made by mixing polystyrene and toluene by using a digital balance with a resolution of 0.001 g. For solutions of large concentration ($w > 0.03$) the relative standard uncertainty of the concentration thus obtained is less than 0.1%. For very dilute solutions ($w < 0.005$) we made larger batch samples so that the relative standard uncertainty of the concentration is always less than 1%. The relative standard uncertainty of the calibration of the balance was checked and found to be less than 0.02% for masses of the order of 200 g. We waited at least 2 h for a full dissolution before loading the sample into the optical cell. Syringes were used for loading the sample and for sucking out bubbles through a TeflonTM tube. After loading the sample, we waited for one to two days for the concentration profile of the solution in the cell to relax to equilibrium before starting measurement. For measurements of samples with the same molecular mass at different concentrations, we used a new solution for each concentration and no dilution from previously used solutions was used. When the samples were changed from one molecular mass to another, we cleaned the cell through many cycles with pure toluene before loading to prevent any polydispersity caused by a residual of a previous sample of different molecular mass.

C. Determination of the S_T and D_c

The basic working equations used for the optical beam-deflection method have been derived in our previous paper.²⁵ By considering the boundary conditions applicable to our sample cell and treating the liquid layer as a one-dimensional liquid layer, we obtained analytic solutions for the temperature gradient ∇T and concentration gradient ∇w in the liquid layer as a function of time, where w is the polymer concentration in terms of the mass fraction of the polymer. The beam-deflection signal Δz is then determined by

$$\Delta z = l_1 \left(\frac{l_1}{2n_1} + \frac{l_2}{n_2} + \frac{l_3}{n_3} \right) \left[\left(\frac{dn}{dT} \right)_{w,p} \nabla T + \left(\frac{dn}{dw} \right)_{T,p} \nabla w \right], \quad (4)$$

where l_1 , l_2 , and l_3 are the path lengths of the polymer solution, the exit window and the air between the exit window and the detector, respectively, n_1 , n_2 , and n_3 are their

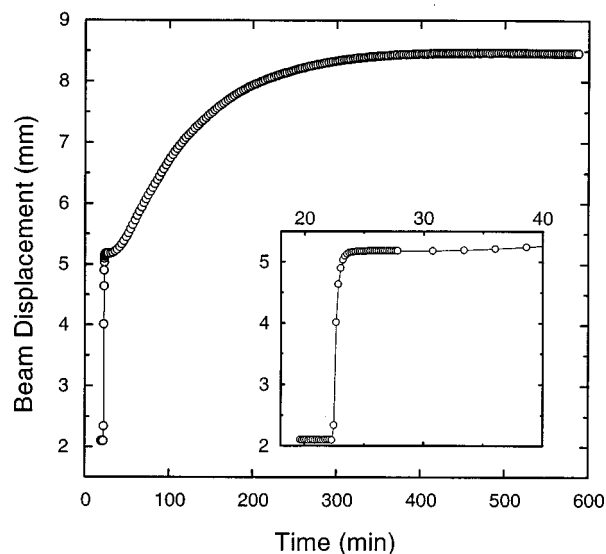


FIG. 2. A typical beam-deflection signal observed from polystyrene solutions in toluene. This curve is from a run with $c = 0.015 \text{ g cm}^{-3}$, $T = 25^\circ\text{C}$, and $p = 1 \text{ atm}$. The initial fast change is the response to the thermal expansion and is sampled at 5 samples/min. The long-time exponential curve corresponds to the thermal diffusion caused by the temperature gradient.

corresponding refractive indices, $(dn/dT)_{w,p}$ is the temperature derivative, and $(dn/dw)_{T,p}$ is the concentration derivative of the refractive index. For polymer solutions, the Lewis number L , that is, the ratio of the collective diffusion coefficient and the thermal diffusivity is very small, $\approx 10^{-4}$. Consequently, the change of the refractive index caused by thermal expansion appears within a few minutes while that caused by thermal diffusion develops over about a day. It is thus a good approximation to replace the temperature gradient term in Eq. (4) with a constant ∇T measured at the boundary of the sample cell, and the dependence of the beam deflection at the time t depends only on the evolution of the concentration gradient as

$$\nabla w = -S_T w(1-w) \nabla T \left\{ 1 - \sum_{m=1}^{\infty} \frac{4}{(2m-1)\pi} \times \sin\left(\frac{(2m-1)\pi}{2}\right) e^{-D_c(2m-1)^2 \pi^2 t/h^2} \right\}, \quad (5)$$

where h is the height of the polymer solution layer and where we have assumed that the beam path is set at the middle height of the liquid layer (see Ref. 25). In practice we need to retain terms only up to $m = 3$ in the summation. In Fig. 2, we present a typical curve of the beam-deflection signal obtained from a polystyrene solution in toluene. As one can see, the refractive-index change caused by thermal expansion appears within a few minutes, while the full development of the thermal-diffusion gradient takes about 10 h. The transient has a smooth exponential curve and finally achieves a steady state with constant concentration gradient. We determined S_T from the total beam deflection at the final steady state corresponding to Eq. (5) in the limit $t \rightarrow \infty$. Subsequently, we fit the entire curve with Eqs. (4) and (5) to obtain D_c . Note that before the concentration diffusion starts to manifest itself

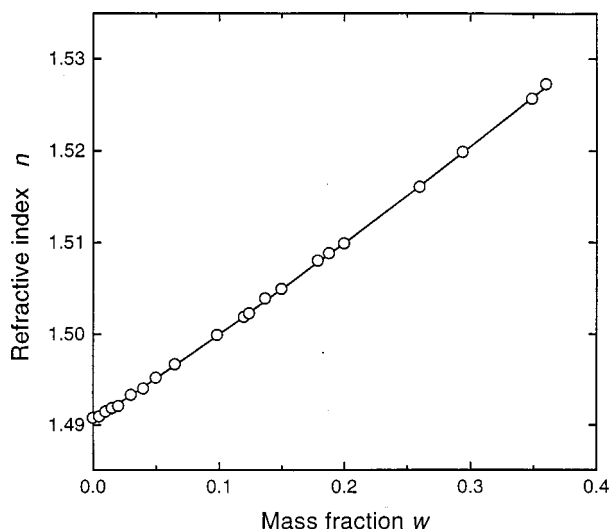


FIG. 3. An example of the measured refractive index of polystyrene solutions in toluene as a function of the concentration. $M_w = 96\,400$. The symbols are measurements at $T = 25^\circ\text{C}$ and the curve represents values calculated from the function given in Table II. Estimated standard uncertainty of the refractive index is $\pm 2 \times 10^{-4}$. The error bars are smaller than the size of the symbols.

there is a short period (≈ 10 min) where the beam deflection curve is flat (Fig. 2 inset). We used this plateau feature to determine the temperature derivative of the refractive index as discussed below.

III. MEASUREMENTS OF THE REFRACTIVE-INDEX DERIVATIVES

In order to evaluate the beam-deflection signal with Eqs. (4) and (5), we measured the concentration derivative and temperature derivative of the refractive index, $(dn/dw)_{T,p}$ and $(dn/dT)_{w,p}$, of the polystyrene solutions in the following two ways.

A. Concentration derivatives $(dn/dw)_{T,p}$

To obtain the concentration derivative $(dn/dw)_{T,p}$ of the refractive index of the polymer solutions, we first measured the refractive index n of the polystyrene solutions in toluene for samples of different molecular masses with an Abbé refractometer²⁶ at constant temperature and pressure. The measured refractive indices for each molecular mass sample

were then fit to a polynomial in the concentration w . We then determined the concentration derivative $(dn/dw)_{T,p}$ by simple differentiation of the polynomials.

The Abbé refractometer was thermostated at $T = 25^\circ\text{C}$ with circulating water and was calibrated with pure water and pure toluene at atmosphere pressure. The polymer solutions with different concentrations were prepared in separate bottles and no dilution from previous samples was used. In Fig. 3 we present an example of the refractive indices measured for samples of molecular mass $M_w = 96\,400$ as a function of the mass fraction w . Each point in Fig. 3 represents an average of six measurements with each two measurements from an individual drop of a sample solution. Estimated standard uncertainty of the refractive index is $\pm 2 \times 10^{-4}$. The second-order power series fits these data with a rms deviation of 1.5×10^{-4} . The relative standard uncertainties of $\pm 1\%$ in the linear coefficient and $\pm 8\%$ in the quadratic coefficient lead to an estimated relative standard uncertainty for the derived $(dn/dw)_{T,p}$ of no more than $\pm 1.4\%$ for up to the maximum concentration of $w = 0.3$ used here. Similar curves were obtained for samples of other molecular masses. The refractive-index data for samples of six different molecular masses overlap at small concentrations and show slight differences at large concentrations. We have fit the refractive-index data separately for each molecular-mass sample and it turns out that the refractive index depends weakly on the molecular mass of the polymer. In Table II, we summarize the fitting results for the refractive index as a function of the mass fraction w of the polymers. We also present the concentration ranges corresponding to the measurements and the fits for the different molecular mass samples. The weak molecular-mass dependence of the refractive index of polymer solutions, associated with the change of partial specific volume of the polymer, has been observed and discussed by Francois *et al.*²⁹ and Candau *et al.*³⁰ Note that the refractive-index function was not measured for the $M_w = 190\,000$ sample. The refractive-index function for this M_w was taken as the simple average of the $M_w = 96\,400$ and $706\,000$ index functions in Table II. The concentration derivatives $(dn/dw)_{T,p}$ we used in this paper were obtained through a direct differentiation of the equations in Table II. These derivatives depend on the concentration of the polymer solution with a weak molecular-mass dependence. The relative standard uncertainties shown are estimated based on the maximum change in refractive index produced in the series of measurements and the index difference resolution of 3

TABLE II. Refractive index of polystyrene solutions in toluene as a function of polymer mass fraction w at $T = 25^\circ\text{C}$ and $p = 1$ atm.

M_w	Refractive index n	Range of w	Uncertainty ^a in $(dn/dw)_{T,p}$
2 630	$1.490\,85 + 0.088\,02w + 0.014\,48w^2$	0–0.50	0.6%
9 100	$1.490\,58 + 0.089\,51w + 0.028\,61w^2$	0–0.57	0.6%
37 400	$1.490\,47 + 0.090\,97w + 0.026\,04w^2$	0–0.50	0.6%
96 400	$1.490\,49 + 0.092\,20w + 0.025\,56w^2$	0–0.36	0.9%
706 000	$1.490\,60 + 0.093\,48w + 0.028\,53w^2$	0–0.11	3%
3 840 000	$1.490\,43 + 0.093\,51w + 0.024\,82w^2$	0–0.055	6%

^aRelative standard uncertainty.

$\times 10^{-4}$. These uncertainties are large enough to be felt in the uncertainty of the measurements of S_T for the highest two molecular-mass samples.

B. Temperature derivative $(dn/dT)_{c,p}$

The temperature derivative of the refractive index $(dn/dT)_{w,p}$ of the polymer solutions determines the magnitude of the initial fast change of the beam deflection caused by thermal expansion. The temperature derivative of the refractive index can be measured separately with a sensitive interferometric method recently developed in our laboratory.³¹ For the polymer solutions we are concerned with here, however, a simpler method can be employed. The mass diffusion coefficient D_c of the polystyrene solutions is four orders of magnitude smaller than D_{th} and, hence, the time of the refractive-index change caused by the thermal expansion is fully separated from that caused by the expansion of the solution. Consequently, we observe a short period before concentration diffusion starts significantly, when the beam deflection is almost flat, as can be seen from the curve in Fig. 2. Calculations with the model equations, Eqs. (4) and (5), for polymer solutions yield the same feature. With our optical cell of 2.92 mm height, the flat part of the signal takes about 10–20 min, and within this time we can take the sample as a homogeneous liquid and the temperature derivative $(dn/dT)_{w,p}$ of the polymer solution at a given concentration can be determined. This method yields $(dn/dT)_{w,p}$ with a relative standard uncertainty no greater than $\pm 2\%$. The relative standard uncertainty in thermal gradient contributes only $\pm 0.7\%$ to the uncertainty in $(dn/dT)_{w,p}$.

Of course, any signal overshoot will invalidate the measurement of $(dn/dT)_{w,p}$ with this method.²⁴ An overshoot of the beam deflection could be caused by an inhomogeneity of the temperature along the horizontal liquid layer, or by overheating when Peltier heater devices were used.²⁴ By controlling the temperature profile along the horizontal liquid layer and by using circulating water for temperature control instead of Peltier devices, we reduced the overshoot of the signal to a negligible level and an initial flat part was obtained for most of the runs.

The resulting values of the temperature derivative $(dn/dT)_{w,p}$, thus determined from beam-deflection signals at $T = 25^\circ\text{C}$, are shown in Fig. 4. With concentrations up to mass fraction 55% of polymer, the measured temperature derivatives of the refractive index show a linear concentration dependence and no observable molecular-mass dependence. $(dn/dT)_{w,p}$ at zero concentration (pure toluene) had already been accurately determined to be $(-5.652 \pm 0.022) \text{ K}^{-1}$ with the present apparatus. A least-squares fit for the slope, over all the data of different molecular masses with the intercept fixed, yields

$$(dn/dT)_{w,p} = -\{(5.652 \pm 0.022) - (1.786 \pm 0.024)w\} \times 10^{-4} \text{ K}^{-1}, \quad (6)$$

with a rms deviation $3 \times 10^{-6} \text{ K}^{-1}$, or $\pm 5\%$. In Fig. 4 the solid line represents the fit to Eq. (6) and the dashed line the values extrapolated from the measurements of Köhler *et al.*^{18,32} However, the measurements of Köhler *et al.* were

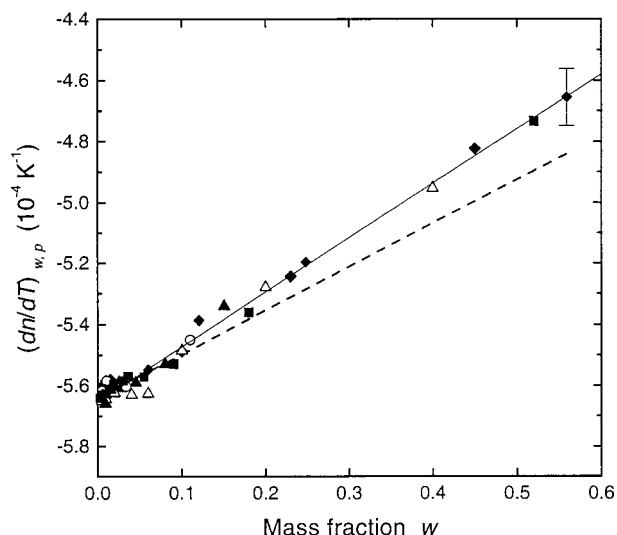


FIG. 4. The temperature derivative of the refractive index as a function of concentration at $T = 25^\circ\text{C}$. The values are determined from the initial response of the beam-deflection curves for samples of different molecular weights. The relative standard uncertainty is estimated to be no greater than $\pm 2\%$. A $\pm 2\%$ error bar is shown. The solid line represents a best fit to Eq. (6). The rms deviation from the linear fit to our data is $\pm 4.7 \times 10^{-6} \text{ K}^{-1}$, or $\pm 0.8\%$. The dashed line represents extrapolated values from a relation by Köhler *et al.* (Ref. 31) obtained for concentrations $c < 0.1 \text{ g cm}^{-3}$. The symbols for different molecular weights are: $M_w = 2630$ (■); 9100 (◇); 37 900 (◆); 96 400 (△); 190 000 (▲); 706 000 (○); 3 840 000 (□).

restricted to concentrations below a mass fraction of 10% of polymer and they are in good agreement with our measurements within the combined experimental standard uncertainties.

IV. MEASUREMENTS OF S_T AND D_c

In this section, we first present the experimental results for S_T and D_c with a brief discussion of the relation between these properties. We then take the product of the two measured properties to obtain D_{th} . It appears that measurements of S_T and D_{th} for polymer solutions in the semidilute regime have not been reported previously.

A. Soret coefficient S_T

We determined S_T of the polystyrene solutions in toluene from the beam deflection at the final steady state using Eqs. (4) and (5). The values of S_T measured at $T = 25^\circ\text{C}$ for polymer samples of seven different molecular masses are presented in Table III as a function of both the mass concentration w and the concentration c . The mass concentration w is the measurement variable and is used in calculating S_T from the working equations. The concentration c is calculated as $c = \rho w$ and is used in the data analysis given below, where ρ is the density of the polymer solutions. We used density data of Scholte³³ for all the samples of different molecular masses, with the assumption that the density is approximately independent of molecular mass. The measured S_T is plotted in Fig. 5 as a function of the concentration c with each point representing an average of 4–6 runs, usually taken at two or three different temperature gradients from 1.5 to 4.5 K/cm. No temperature-gradient dependence of the

TABLE III. Soret coefficient and diffusion coefficient of polystyrene solutions in toluene measured at $T=25^\circ\text{C}$.

w	c (g cm $^{-3}$)	S_T (K $^{-1}$) ^a	D_c (10 $^{-7}$ cm $^{-2}$ s $^{-1}$)
$M_w=2630$			
0.009 0	0.007 8	0.0333 \pm 0.0010	31.9 \pm 0.5
0.029 0	0.025 1	0.0327 \pm 0.0009	32.2 \pm 0.6
0.036 0	0.031 3	0.0327 \pm 0.0007	32.3 \pm 0.5
0.090	0.079	0.0313 \pm 0.0006	33.2 \pm 0.6
0.180	0.161	0.0286 \pm 0.0004	34.5 \pm 0.5
0.520	0.501	0.0201 \pm 0.0003	39.4 \pm 0.6
$M_w=9100$			
0.010 0	0.008 6	0.0640 \pm 0.0007	18.1 \pm 0.4
0.024 0	0.020 8	0.0625 \pm 0.0005	18.4 \pm 0.3
0.060	0.052 4	0.0567 \pm 0.0005	19.6 \pm 0.4
0.120	0.106 1	0.0490 \pm 0.0003	21.7 \pm 0.4
0.248	0.225	0.0340 \pm 0.0002	26.2 \pm 0.3
0.559	0.543	0.0210 \pm 0.0004	36.4 \pm 0.4
$M_w=37\,900$			
0.006 0	0.005 18	0.118 \pm 0.002	9.2 \pm 0.2
0.010 0	0.008 64	0.114 \pm 0.002	9.5 \pm 0.2
0.015 0	0.013 0	0.110 \pm 0.001	9.8 \pm 0.1
0.035	0.030 4	0.0965 \pm 0.0006	11.14 \pm 0.14
0.100	0.088	0.0694 \pm 0.0008	15.0 \pm 0.2
0.230	0.208	0.0402 \pm 0.0003	21.7 \pm 0.2
0.450	0.427	0.0265 \pm 0.0003	31.0 \pm 0.7
$M_w=96\,400$			
0.002 5	0.002 16	0.226 \pm 0.004	4.95 \pm 0.07
0.005 0	0.004 31	0.215 \pm 0.002	5.15 \pm 0.08
0.007 5	0.006 47	0.210 \pm 0.002	5.37 \pm 0.08
0.010 0	0.008 64	0.190 \pm 0.002	5.65 \pm 0.12
0.015 0	0.013 0	0.1784 \pm 0.0014	6.01 \pm 0.09
0.020	0.017 3	0.167 \pm 0.001	6.51 \pm 0.15
0.025	0.021 7	0.157 \pm 0.002	6.95 \pm 0.13
0.040	0.034 8	0.133 \pm 0.001	7.97 \pm 0.11
0.060	0.052 4	0.109 \pm 0.001	9.65 \pm 0.15
0.100	0.088	0.0797 \pm 0.0003	12.5 \pm 0.2
0.200	0.178	0.0495 \pm 0.0011	19.0 \pm 0.3
0.400	0.375	0.0297 \pm 0.0006	28.4 \pm 0.5
$M_w=190\,000$			
0.009	0.007 8	0.241 \pm 0.004	4.00 \pm 0.05
0.015	0.013 0	0.221 \pm 0.003	4.55 \pm 0.08
0.025	0.021 7	0.182 \pm 0.002	5.48 \pm 0.09
0.045	0.039 2	0.1364 \pm 0.0009	7.39 \pm 0.14
0.080	0.070 1	0.0901 \pm 0.0008	10.53 \pm 0.12
0.148	0.132	0.0616 \pm 0.0005	14.9 \pm 0.2
$M_w=706\,000$			
0.005 48	0.004 73	0.424 \pm 0.008	2.40 \pm 0.04
0.110	0.009 5	0.323 \pm 0.005	3.18 \pm 0.04
0.020	0.017 3	0.236 \pm 0.002	4.30 \pm 0.06
0.033 7	0.029 3	0.173 \pm 0.002	5.8 \pm 0.1
0.110	0.097 0	0.0805 \pm 0.0008	12.3 \pm 0.2
$M_w=3\,840\,000$			
0.002 5	0.002 16	0.760 \pm 0.015	1.24 \pm 0.04
0.005 0	0.004 31	0.550 \pm 0.011	1.77 \pm 0.06
0.009 0	0.007 77	0.408 \pm 0.006	2.41 \pm 0.06
0.013	0.011 2	0.335 \pm 0.003	2.98 \pm 0.08
0.019	0.016 4	0.260 \pm 0.003	3.85 \pm 0.07
0.030	0.026 0	0.190 \pm 0.005	5.19 \pm 0.09
0.055	0.048 0	0.1285 \pm 0.0014	7.6 \pm 0.1

^aThe additional uncertainty in S_T due to the uncertainty of the $(dn/dw)_{T,p}$ listed in Table II is not included here.

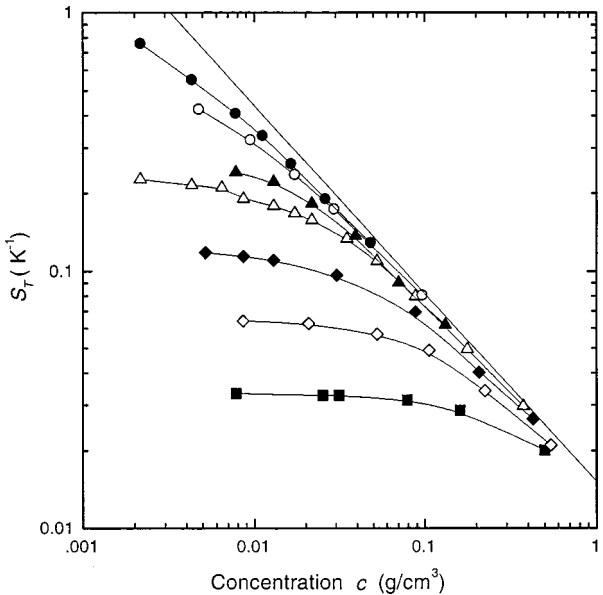


FIG. 5. Soret coefficient of polystyrene solutions in toluene for samples of different molecular weights at $T=25^\circ\text{C}$. The curves represent spline fits of the data. The straight line is the graphically estimated asymptote of the form Eq. (7) with exponent $x_T=0.73\pm0.03$. The relative standard uncertainty over most of the concentration range is less than $\pm 2\%$ but increases to $\pm 3\%$ at the lowest concentrations. The square symbol size corresponds to a vertical error bar of $\pm 4\%$. The symbols for different molecular weights are: $M_w=2630$ (■); 9100 (◇); $37\,900$ (◆); $96\,400$ (△); $190\,000$ (▲); $706\,000$ (○); $3\,840\,000$ (●).

measured S_T was observed. The relative standard uncertainty of our measurements at most concentrations is less than $\pm 2\%$ except at very dilute solutions where the relative standard uncertainty increases to $\pm 3\%$. The additional relative standard uncertainty for S_T due to the uncertainty of the $(dn/dw)_{T,p}$ listed in Table II is not included in Table III or Fig. 5 in order to display the resolution of the concentration dependence of S_T .

As the concentration increases, S_T becomes independent of the molecular mass and depends only on the concentration; it is well approximated by a power-law

$$S_T \sim \left(\frac{c}{c^*} \right)^{-x_T}. \quad (7)$$

A graphical fit of Eq. (7) as an asymptote to the measured data yields an apparent exponent $x_T=0.73\pm0.03$. Although the apparent value of the exponent x_T should reflect the limited concentration range considered, the exponent value obtained is reasonably close to the value $x_D=0.77$ predicted for the collective diffusion coefficient from Eq. (3). Below we shall fit our data to a more general crossover expression which is consistent with the theoretically expected exponent so that the somewhat lower effective exponent can be rationalized as a crossover effect.

In the dilute regime the measured S_T depends strongly on the molecular mass and decreases linearly as a function of concentration for each molecular mass. To describe the concentration dependence of S_T in the dilute regime we extrapolate the measured data to zero concentration and fit the data with the following virial expansion:

$$S_T = S_{T0} [1 - k_S c + O(c^2)], \quad (8)$$

TABLE IV. Infinite dilution Soret coefficient S_{T0} and leading virial coefficient k_S of polystyrene solutions in toluene. See Figs. 6 and 7.

M_w (g mol ⁻¹)	S_{T0} (K ⁻¹) ^a	k_S (cm ³ g ⁻¹)
2 630	0.034±0.001	1.03±0.24
9 100	0.0658±0.0007	2.6±0.3
37 900	0.124±0.002	9.3±0.8
96 400	0.240±0.004	23±5
190 000	0.276±0.004	15.7±4.7
706 000	0.52±0.03	40±6
3 840 000	0.97±0.07	101±15

^aRelative standard uncertainties in S_{T0} given here include the uncertainties in $(dn/dw)_{T,p}$ shown in Table II.

where k_S is the leading virial coefficient of S_T , and S_{T0} is the infinite-dilution Soret coefficient. The results for S_{T0} and for the virial coefficient k_S are presented in Table IV, with a relative standard uncertainty of $\pm 1\%$ to $\pm 7\%$ for S_{T0} and $\pm 9\%$ to $\pm 30\%$ for k_S . The molecular-mass dependence of S_{T0} is plotted in Fig. 6 and our data are described by the power-law:

$$S_{T0} = b_S M_w^{\nu_S}, \quad (9)$$

with amplitude $b_S = (8.2 \pm 1.5) \times 10^{-4}$ (K⁻¹) and exponent $\nu_S = 0.48 \pm 0.02$. The uncertainties here are one standard uncertainty and are the estimates from the Marquardt least-squares fitting algorithm, which assumes uncorrelated uncertainties in the fitting parameters. We note that ν_S is slightly smaller than the corresponding exponent $\nu_D = 0.53 \pm 0.02$ for the infinite-dilution diffusion coefficient exponent estimated in the next section, but the range of previous measurements of the diffusion coefficient exponent overlaps with the range for ν_S so it not clear if this discrepancy is statistically significant. In Fig. 6, we also present results extrapolated from the measurements of Köhler *et al.*¹⁸

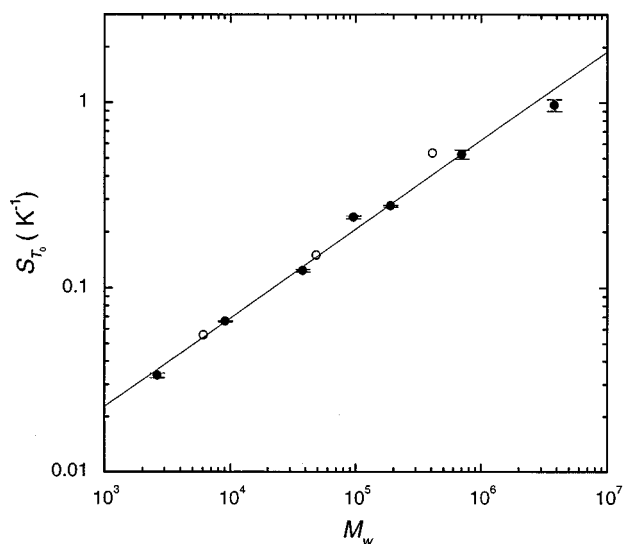


FIG. 6. Values of the Soret coefficient S_{T0} at infinite dilution for solutions of different molecular weight samples from Table IV. Relative standard uncertainty is estimated to be $\pm 2\%$ from fitting to the linear form, Eq. (8). The symbol heights correspond to an uncertainty of $\pm 4\%$. The solid line represents the power-law fit to our data, Eq. (9), with amplitude $(8.2 \pm 1.5) \times 10^{-4}$ (K⁻¹) and exponent $\nu_S = 0.48 \pm 0.02$. (●)—This work; (○)—Köhler *et al.* (Ref. 18).

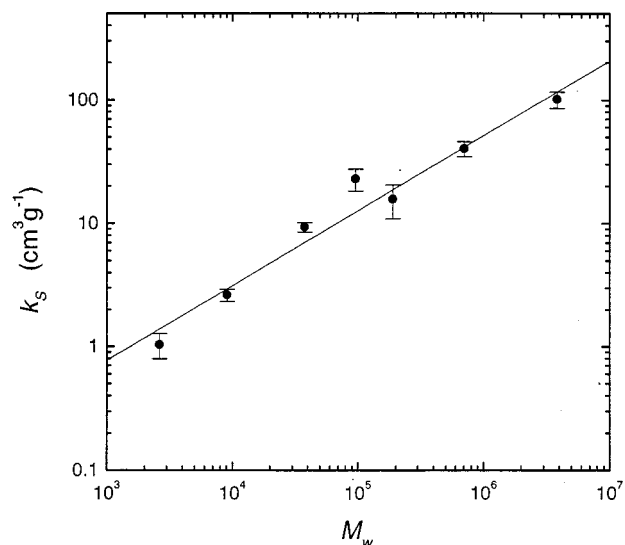


FIG. 7. Leading virial coefficient k_S of the Soret coefficient in the dilute region as a function of the molecular weight, obtained from fits to Eq. (8). The data are from Table IV. Relative standard uncertainty is estimated to be from $\pm 3\%$ to $\pm 29\%$ from fitting to the linear form, Eq. (8). The solid line represents the power-law fit to our data, Eq. (10), with an amplitude $(1.16 \pm 0.6) \times 10^{-2}$ (cm³ g) and an exponent $a_S = 0.61 \pm 0.04$.

The virial coefficient k_S for the dilute concentration regime also exhibits a power-law dependence on the molecular mass as shown in Fig. 7 and can be fitted to the power-law

$$k_S = b_{kS} M_w^{a_S}. \quad (10)$$

Our data yield an amplitude $b_{kS} = (1.18 \pm 0.6) \times 10^{-2}$ (cm³ g⁻¹) and an exponent $a_S = 0.61 \pm 0.04$. The standard uncertainties here are the estimates from the Marquardt least-squares fitting algorithm. This exponent can be compared with the exponent 0.74 for the molecular-mass dependence of the intrinsic viscosity $[\eta]$ of polystyrene in toluene at 25 °C and the exponent 0.78–0.79 for the molecular dependence of $A_2 M_w$ at 25 °C, where A_2 is the second virial coefficient.^{34,35} These scaling relations are helpful in identifying the most suitable reducing concentration variables for S_T in the absence of a complete theory of the concentration dependence of the transport properties of polymer solutions.

B. Collective diffusion coefficient D_c

From the same beam-deflection measurements described above we can also obtain D_c . The diffusion coefficients determined with Eqs. (4) and (5) for samples of seven different molecular masses at mean temperature of 25 °C are presented in Table III, and are plotted as a function of the concentration c in Fig. 8. The general features of the concentration dependence of the diffusion coefficient are in agreement with those obtained by previous investigators from light scattering.^{12,13} Our experiments with an optical-beam deflection method, however, yield a smaller uncertainty for the measured D_c and thus a smaller uncertainty in the exponent value discussed below. The maximum spread of the measured D_c of different runs is $\pm 4\%$, which characterizes the

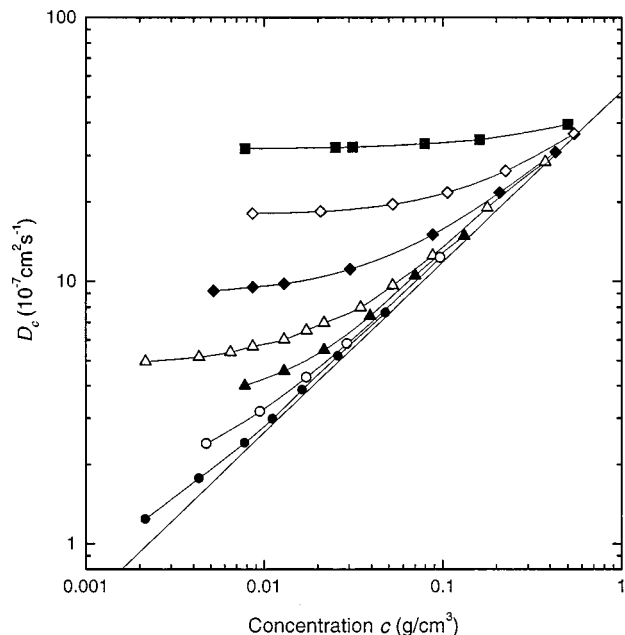


FIG. 8. Diffusion coefficients of polystyrene solutions in toluene for samples of different molecular weights at $T=25^\circ\text{C}$. The curves represent spline fits to the data. The straight line represents a graphical asymptote with exponent $x_D=0.65\pm0.02$. The relative standard uncertainties of the data are $\pm 3\%$ and the diamond data symbols are about $\pm 4\%$ high. The data are from Table III. The symbols for different molecular weights are: $M_w=2630$ (■); 9100 (◇); 37 900 (◆); 96 400 (△); 190 000 (▲); 706 000 (○); 3 840 000 (●).

relative standard uncertainty of the measured D_c . The relative standard uncertainty of the mean D_c is usually less than $\pm 2\%$.

In the semidilute region, D_c shows asymptotic power-law dependence as expressed by Eq. (3). The concentration exponent we obtained by graphical estimation from the measured data is $x_D=0.65\pm0.02$, in agreement with results reported by several authors.^{11–13} The relative standard uncertainty estimate here is the range of exponents which would give a graphically acceptable asymptote. Brown and Nicolai⁷ suggested that much of the existing D_c data (where corrections to experimental data have not been made) for flexible polymers could be fitted to an exponent 0.70 which is close to the theoretical prediction Eq. (3) if a correction for the “backflow” effect is employed. Since the identification of the collective friction coefficient with a translational friction coefficient on which this correction is based seems debatable, we have avoided introducing such a correction here. The alternative correction by Geissler and Hecht¹⁴ seems reasonable, but requires data for the translational diffusion coefficient of toluene in the polystyrene/toluene solutions at the D_c measurement temperature. Such data are unavailable for the temperature and molecular masses used in our experiment.

In the dilute regime, D_c can be described by the virial expansion, Eq. (1). By fitting the data at each molecular mass to Eq. (1) we obtain the infinite-dilution diffusion coefficient D_{c0} and the leading virial coefficient k_D . The results are presented in Table V with a standard deviation of $\pm 2\%$ to $\pm 28\%$ for the two coefficients. D_{c0} is plotted in Fig. 9

TABLE V. Infinite dilution diffusion coefficient D_{c0} and leading virial coefficient k_D of polystyrene solutions in toluene. See Figs. 9 and 10.

M_w (g mol ⁻¹)	D_{c0} (10 ⁻⁷ cm ² s ⁻¹)	k_D (cm ³ g ⁻¹)
2 630	31.74 \pm 0.5	0.58 \pm 0.04
9 100	17.72 \pm 0.4	2.1 \pm 0.2
37 900	8.75 \pm 0.2	9.9 \pm 1.4
96 400	4.714 \pm 0.08	22 \pm 2
190 000	3.15 \pm 0.08	34.2 \pm 1.0
706 000	1.63 \pm 0.11	100 \pm 12
3 840 000	0.707 \pm 0.14	347 \pm 96

against the molecular mass of polystyrene and compared with the values extrapolated from Köhler *et al.*¹⁸ A power-law fit to our data yields

$$D_{c0}=b_D M_w^{-\nu_D}, \quad (11)$$

with an amplitude of $b_D=(2.19\pm0.29)\times 10^3$ (cm² s⁻¹) and an exponent $\nu_D=0.53\pm0.02$. The standard uncertainties here are the estimated by the Marquardt least-squares fitting algorithm. The exponent value is in agreement with the earlier measurement³⁶ of ν_D for polystyrene in the good solvent benzene, $\nu_D=0.55\pm0.02$. The molecular-mass dependence of the linear coefficient k_D is shown in Fig. 10 and can be represented by the power-law:

$$k_D=b_{kD} M_w^{a_D}. \quad (12)$$

The fitted amplitude is $b_{kD}=(4.2\pm1.2)\times 10^{-4}$ (cm³ g⁻¹) and the fitted exponent is $a_D=0.93\pm0.06$. This exponent value may be compared to the literature values^{12,37–39} which exhibit a disturbingly large range from 0.44 to 1.1. The standard uncertainties here are the estimates from the Marquardt least-squares fitting algorithm.

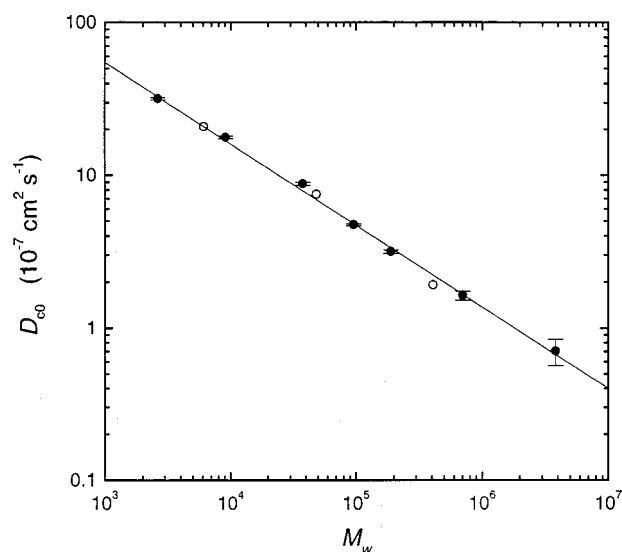


FIG. 9. Values of the diffusion coefficient D_{c0} at infinite dilution for solutions of different molecular weight samples. Relative standard uncertainties are estimated to be $\pm 1\%$ from fitting to the linear form, Eq. (8). The solid line is the power-law fit to our data, Eq. (11), yielding an amplitude $(2.19\pm0.29)\times 10^3$ (cm² s⁻¹) and an exponent $\nu_D=0.53\pm0.02$. The data are from Table V. (●)—This work; (○)—Köhler *et al.* (Ref. 18).

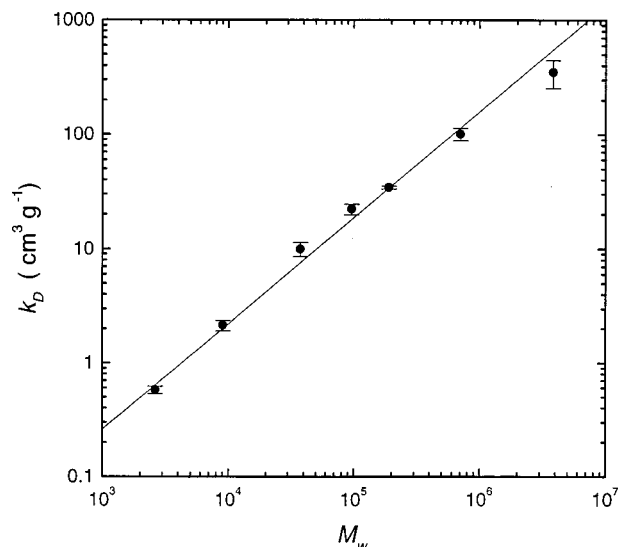


FIG. 10. Leading virial coefficient k_D of the diffusion coefficient in the dilute region as a function of the molecular weight, obtained from fits to Eq. (1). Relative standard uncertainties are estimated to be $\pm 16\%$ from fitting to the linear form, Eq. (8). The solid line represents the fit to our data, Eq. (12), yielding an amplitude $(4.2 \pm 1.2) \times 10^{-4} \text{ (cm}^3 \text{ g}^{-1})$ and an exponent $a_D = 0.93 \pm 0.02$.

Several points in Figs. 6, 7, 9, and 10 lie off the power-law fit by more than their estimated standard uncertainty. We believe this is due to having insufficient data points at low concentrations to reach accurate fitted linear virials such as Eqs. (8) and (1). This is particularly evident at the $M_w = 96\,400$ point in Fig. 7. This molecular mass had a large number of concentration points measured including two concentrations below 0.005 g/cm^3 . The result is a higher slope, k_S , but which does not appear to agree with the other measurements.

C. Thermal-diffusion coefficient D_{th}

With the measured S_T and D_c we can determine the thermal-diffusion coefficient, $D_{th} = S_T D_c$. The D_{th} thus obtained are shown in Fig. 11 on a log-log scale (top) and on

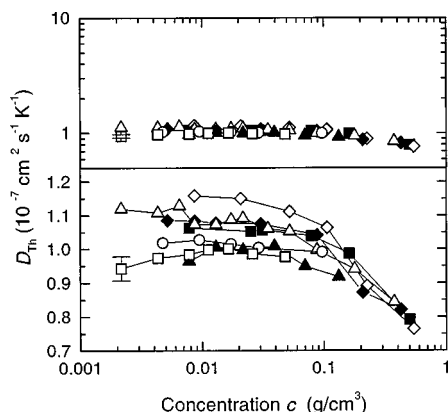


FIG. 11. The thermal-diffusion coefficient $D_{th} = S_T D_c$ of polystyrene solutions in toluene. The top part is on a log-log scale and the bottom part on a linear-log scale. The relative standard uncertainties are between $\pm 2\%$ and $\pm 4\%$. A 4% error bar is shown. The symbols are: $M_w = 2630$ (■); 9100 (◇); 37 900 (◆); 96 400 (△); 190 000 (▲); 706 000 (○); 3 840 000 (□).

a linear-log scale (bottom). In the dilute regime, D_{th} is independent of concentration within the relative standard uncertainty of around $\pm 3\%$. In the semidilute regime, however, the data show a weak but observable concentration dependence, as determined by the difference of the fitted apparent exponents for S_T and for D_c in the semidilute region, $x_T - x_D = 0.73 - 0.65 = 0.08 \pm 0.03$.

Measurements obtained earlier by Meyerhoff and Nachtigall¹⁶ and recently by Ecenarro *et al.*¹⁷ for polystyrene solutions in toluene in the dilute regime showed that D_{th} decreases as the concentration increases and D_{th} is independent of molecular mass. The thermal-diffusion coefficient measured by Ecenarro *et al.* at concentration $c = 0.025 \text{ g cm}^{-3}$ is about $0.85 \text{ cm}^2 \text{ s}^{-1} \text{ K}^{-1}$. In contrast, the measurement of Köhler *et al.*¹⁸ showed that D_{th} at that concentration to be close to $1.1 \text{ cm}^2 \text{ s}^{-1} \text{ K}^{-1}$. Our experimental results in the entire dilute regime are independent of the concentration and agree with those of Köhler *et al.*¹⁸ within our experimental relative standard uncertainties of 2%–4%. The thermal-diffusion coefficient of polymer solutions in the semidilute region, however, has not been reported previously in the literature to our knowledge.

Giddings *et al.*^{19,20} have measured D_{th} of polystyrene solutions in toluene in the limit of infinitely dilute concentration by using a thermal-field flow-fractionation technique. Their experimental values for D_{th} are independent of the molecular mass and of the chain topology of the polystyrene molecules. Within the combined experimental relative standard uncertainties of the two experiments of $\pm 7\%$, our dilute solution measurements agree with the measurements of Giddings *et al.*¹⁹ Furthermore, our data show that D_{th} is also insensitive to the molecular mass in both the dilute and semidilute regimes. Brochard and de Gennes rationalized the independence of D_{th} from the molecular mass as due to a lack of long-range correlation between monomers.²¹ More theoretical work is desirable to understand the concentration as well as the molecular-mass dependence of D_{th} in the semidilute regime.

D. Effect of polydispersity on S_T , D_c , and D_{th}

As can be seen from Table I, the polystyrene samples used in our experiments to measure S_T and D_c have a polydispersity varying from 1% to 5%. Hence, the question arises to what extent these deviations from monodispersity may affect the values obtained for S_T and D_c . We note that the thermal diffusion coefficient D_{th} is essentially independent of molecular mass and that the coefficients S_T and D_c become insensitive to molecular mass at semidilute and higher concentrations. Thus, the largest effect of any polydispersity should arise in measurements of S_T and D_c obtained in the dilute solution regime. We expect that the polydispersity effects in our thermal-gradient measurements will be similar to those in forced Rayleigh scattering measurements, where the concentration gradients are induced by a sinusoidal temperature pattern. Hence the polydispersity corrections derived by Rossmanith and Köhler⁴⁰ for forced Rayleigh measurements in dilute polymer solutions provide an estimate of the effect of polydispersity on our measurements as well. These cor-

rections should be an upper bound to the effect of polydispersity for any concentration. Given the molecular mass scaling laws for S_T and D_c in the dilute limit, Eqs. (9) and (10), respectively, the ratio of mass weighted to number weighted properties are given to lowest order by

$$\langle S_T \rangle_w / \langle S_T \rangle_n = 1 - \nu_s (M_w / M_n - 1), \quad (13)$$

and

$$\langle D_{c0} \rangle_w / \langle D_{c0} \rangle_n = 1 + \nu_D (M_w / M_n - 1), \quad (14)$$

where the subscripts w and n refer to mass and number averaging and the constants ν_s and ν_D are the mass scaling exponents for S_T and D_c . For values of M_w / M_n ranging from 1.01 to 1.05 (see Table I) we then calculate an apparent shift in S_T ranging from -0.5% to -2.4% from a number averaged S_T and a shift ranging from $+0.5\%$ to $+2.6\%$ in the apparent value of D_c . These effects are within the estimated relative standard uncertainties of our experimental data and no polydispersity corrections have been applied to the experimental values presented in Tables III–V.

V. MASTER CURVE DESCRIBING THE CONCENTRATION DEPENDENCE OF S_T AND D_c

In recent years there have been efforts to describe the static and dynamic properties of polymer solutions by using scaling and renormalization-group (RG) methods^{1,2,41–46} similar to those successfully employed to describe critical phenomena. These efforts have been motivated by the success of scaling arguments to describe static polymer-solution properties such as the inverse of the osmotic compressibility $(d\Pi/dc)_{T,p}$ and the static correlation length ξ_s . For these static properties, it was found^{7,12,47} from RG theory that the reduced concentration X_S is related to the osmotic virial coefficient A_2 , by the equation $X_S = (16/9)A_2M_w c$ and measurements of scaling curves for these properties corresponded rather well to theoretical expectations.⁷

The situation for dynamic properties is less satisfactory, however. The RG calculations of Shiwa *et al.*^{43,44} indicate that X_S is the reduced concentration variable for D_c and that $k_D = 0$ at the theta point where the osmotic second virial coefficient vanishes [$A_2(T = \theta) = 0$]. Wiltzius *et al.*¹² have shown, however, that X_S is not a reducing variable for D_c , at least for polystyrene in various solvents, and it is well known that k_D is quite negative at the theta point.^{4–6,8} On a more positive side, Wiltzius *et al.*¹² noted that a universal summary of polystyrene data could be obtained by using k_{DC} as the reducing concentration variable. This finding is natural given the common utilization of $c[\eta] = c/c^*$ as a reducing variable for the viscosity of polymer solutions. Recent RG calculations by Cherayil and Freed⁴⁶ of k_D for ideal polymer solutions (i.e., at the theta point) indicate that $k_D = -1.06[\eta]$, in reasonable accord with experiments which indicate a prefactor nearer -0.7 or -0.8 (see discussion in Ref. 46).

Although there is no fully acceptable theory of the concentration dependence of D_c at nonvanishing concentration, we can develop a reasonable phenomenological description based on the observations of Wiltzius *et al.*¹² mentioned above and on the preliminary RG calculations by Shiwa

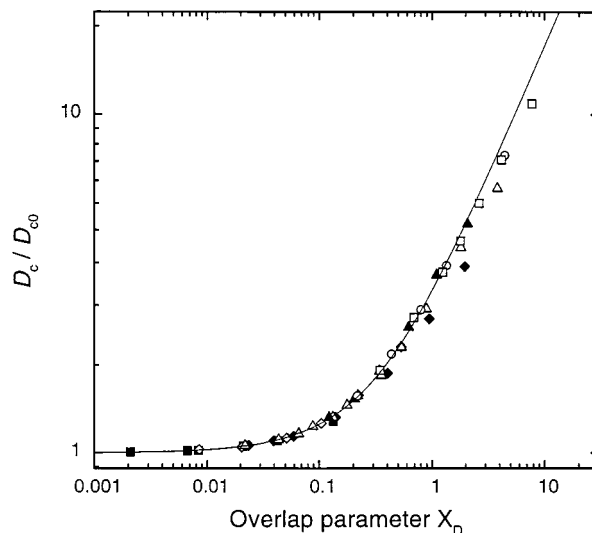


FIG. 12. Reduced diffusion coefficient D_c / D_{c0} as a function of the reduced concentration $X_D = 0.46(k_{DC})$, with D_{c0} and k_D given in Table V. The solid curve represents values calculated from Eq. (15) with $A_D = 2.71$. The square symbol size corresponds to a vertical error bar of $\pm 4\%$. The symbols for different molecular weights are: $M_w = 2630$ (■); 9100 (◇); 37900 (◆); 96400 (△); 190000 (▲); 706000 (○); 3840000 (□).

*et al.*⁴³ We take as the scaling variable $X_D = r_D(k_{DC})$, where r_D is a proportionality factor to be determined from the data. We use the very simple scaling equation following Nystrom and Roots⁴¹ in adapting the scaling form from Shiwa⁴⁴ to give the approximant:

$$\frac{D_c}{D_{c0}} = \frac{1 + A_D X_D (1 + X_D)^B}{(1 + X_D)^A}, \quad (15)$$

with $A = (\nu - 1)/(3\nu - 1)$, $B = (2 - 3\nu)/(3\nu - 1)$, and $A_D = A + r_D^{-1}$. With these exponents A and B , the scaled diffusivity will satisfy Eq. (3) for x_D for large concentrations and the condition on A_D assures that the leading virial coefficient k_D is recovered at low concentrations. Here we take $\nu = 0.588$ yielding the exponents $A = 0.539$ and $B = 0.309$. We have reduced the data for D_c from Table III by using the results from Table V and have done a Marquardt least-squares fit for the proportionality constant r_D . The resulting scaling is shown in Fig. 12. The proportionality constant is found to be $r_D = 0.46 \pm 0.02$ with the resulting coefficient $A_D = 2.7 \pm 0.1$. This scaling seems to work within the experimental relative standard uncertainties for all but the $M_w = 37900$ data, which show (Fig. 10) a deviation outside the relative standard uncertainty estimate from the power-law line.

The same argument with the reducing concentration variable $X_S = r_S(k_S c)$ yields a reduction of our Soret-coefficient data of the same form:

$$\frac{S_{T0}}{S_T} = \frac{1 + A_S X_S (1 + X_S)^B}{(1 + X_S)^A}. \quad (16)$$

with $A_S = A + r_S^{-1}$ as demonstrated in Fig. 13. Note that we are using the same exponents A and B in Eqs. (15) and (16). For Fig. 13 it was necessary to use the fitted Eq. (10) to calculate k_S , because of the relatively large deviations of k_S from the expected form (see Fig. 7). We find $r_S = 3.6 \pm 0.2$

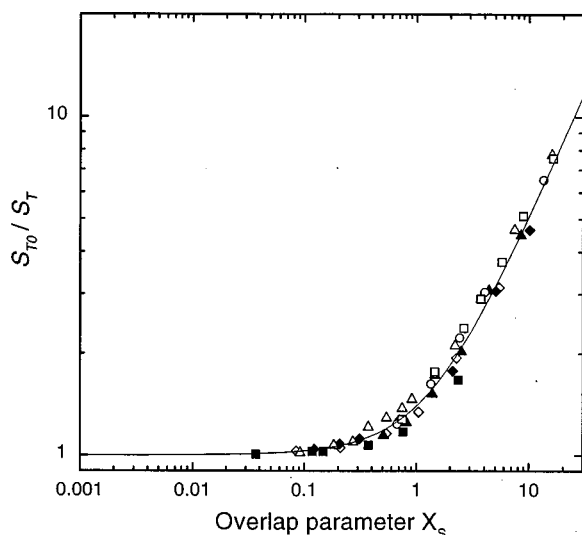


FIG. 13. Reduced Soret coefficient S_{T0}/S_T as a function of the reduced concentration $X_S = 3.65(k_S c)$, with S_{T0} given in Table IV. Here k_S is calculated from the fitted power law of Fig. 7. The solid curve represents values calculated from Eq. (16) with $A_S = 0.813$. The estimated relative standard uncertainties range from $\pm 2\%$ to $\pm 23\%$ for these data; the square symbol size corresponds to a vertical error bar of $\pm 4\%$. The symbols for different molecular weights are: $M_w = 2630$ (■); 9 100 (◇); 37 900 (◆); 96 400 (△); 190 000 (▲); 706 000 (○); 3 840 000 (□).

with a resulting coefficient $A_S = 0.83 \pm 0.05$. Since the molecular-mass dependence of k_S is very similar to that found for $[\eta]$ and $A_2 M_w$, we would expect that replacing $A_2 M_w$ by k_S should lead to a good reduction.

The concentration exponents x_D and x_T implied by Eqs. (15) and (16) for large X_D and X_S are $x_D = x_T = 0.77$ in agreement with the theoretical estimate of this exponent $x_D = x_T = \nu/(3\nu - 1)$ as mentioned in Sec. I. The simple approximants of Eqs. (15) and (16) have the scaling-theory limit of Eq. (3) built into them by construction. Since our measured S_T and D_c data are consistent with these expressions, the apparent values of the concentration exponents x_D and x_T discussed in previous sections are consistent with the existence of a broad concentration crossover regime where the apparent exponents are smaller than their asymptotic values.

It seems theoretically unclear to us why the molecular-mass dependence of the reduced concentration variable k_{DC} for D_c should deviate so strongly from the expectations of RG theory,⁴⁵ while the molecular-mass dependence of the reduced concentration variable k_{SC} for S_T accords rather well with the expected mass scaling. Stated otherwise, k_{SC} is approximately proportional to X_S (see the discussion above), but k_{DC} is not proportional to X_S as predicted by RG theory calculations for polymers in good solvents.⁴⁵ Further RG calculations of the excluded volume dependence of k_D might clarify this discrepancy.

VI. CONCLUSION

By using an optical beam-deflection method with the apparatus recently developed in our laboratory we have measured the Soret coefficient S_T and the collective diffusion coefficient D_c of solutions of linear polystyrene in the good-

solvent toluene in the dilute and semidilute concentration regimes and over a large range of molecular masses. From fitting the experimental data, we obtained a set of power-law exponents characterizing the infinite-dilution values of S_T and D_c and their leading virial coefficients, k_S and k_D . In the semidilute regime, the measured S_T exhibit power-law scaling with polymer concentration and are found to be independent of the molecular mass of the polymer. The measured S_T and D_c as a function of concentration and molecular mass can be well fitted by an interpolation function suggested by Shiwa,⁴⁵ where the reduced concentration variable is defined phenomenologically in terms of the leading concentration virial coefficient for that property. Our observations invite further theoretical studies to explain these striking experimental regularities.

ACKNOWLEDGMENT

This research is supported at the University of Maryland by NSF Grant No. CHE-9805260. Certain commercial materials and instruments are identified in this article to adequately specify the experimental procedure. In no case does such identification imply recommendation or endorsement by the National Institute of Standards and Technology, nor does it imply that materials or equipment identified are necessarily the best available for the purpose.

- ¹P. G. de Gennes, *Scaling Concepts in Polymer Physics* (Cornell University Press, Ithaca, NY, 1979).
- ²K. F. Freed, *Renormalization Group Theory of Macromolecules* (Wiley, New York, 1987).
- ³H. Yamakawa, *Modern Theory of Polymer Solutions* (Harper & Row, New York, 1971).
- ⁴C. C. Han and A. Z. Akcasu, *Polymer* **22**, 1165 (1981).
- ⁵P. M. Cotts and J. Selser, *Macromolecules* **23**, 2050 (1990).
- ⁶K. Huber, S. Bantle, P. Lutz, and W. Burchard, *Macromolecules* **18**, 1461 (1985).
- ⁷W. Brown and T. Nicolai, *Colloid Polym. Sci.* **268**, 977 (1990).
- ⁸A. Kolodenko and J. F. Douglas, *Phys. Rev. E* **51**, 1081 (1995).
- ⁹According to ISO 31-8 the term "molecular weight" has been replaced by the technically more correct term "relative molecular mass." The older, more conventional, notation for number and weight-average molecular weights is utilized in the present paper.
- ¹⁰M. Daoud, J. P. Cotton, B. Farnoux, G. Jannink, G. Sarma, H. Benoit, R. Duplessix, C. Picot, and P. G. de Gennes, *Macromolecules* **8**, 804 (1975).
- ¹¹M. Adam and M. Delsanti, *Macromolecules* **10**, 1229 (1997).
- ¹²P. Wiltzius, H. R. Haller, D. S. Cannell, and D. W. Schaefer, *Phys. Rev. Lett.* **53**, 834 (1984).
- ¹³N. Nemoto, Y. Makita, Y. Tsunashima, and M. Kurata, *Macromolecules* **17**, 2629 (1984).
- ¹⁴E. Geissler and A. M. Hecht, *J. Phys. (France) Lett.* **39**, 631 (1978).
- ¹⁵T. P. Lodge, *J. Phys. Chem.* **97**, 1480 (1993).
- ¹⁶G. Meyerhoff and K. Nachtigall, *J. Polym. Sci.* **57**, 227 (1962).
- ¹⁷O. Eceñarro, J. A. Madariaga, J. L. Navarro, C. M. Santamaría, J. A. Carrión, and J. M. Savirón, *Macromolecules* **27**, 4968 (1994).
- ¹⁸W. Köhler, C. Rosenauer, and P. Rossmanith, *Int. J. Thermophys.* **16**, 11 (1995).
- ¹⁹J. C. Giddings, K. D. Caldwell, and M. N. Myers, *Macromolecules* **9**, 106 (1976).
- ²⁰M. E. Schimpf and J. C. Giddings, *Macromolecules* **20**, 1561 (1987).
- ²¹F. Brochard and P. G. de Gennes, *C. R. Acad. Sci. Paris* **293**, Serie II, 1025 (1981).
- ²²M. Giglio and A. Vendramini, *Phys. Rev. Lett.* **34**, 561 (1975).
- ²³M. Giglio and A. Vendramini, *Phys. Rev. Lett.* **38**, 26 (1977).
- ²⁴P. Kolodner, H. Williams, and C. Moe, *J. Chem. Phys.* **88**, 6512 (1988).
- ²⁵K. J. Zhang, M. E. Briggs, R. W. Gammon, and J. V. Sengers, *J. Chem. Phys.* **104**, 6881 (1996).

- ²⁶J. Reilly and W. N. Rae, *Physico-Chemical Methods* (Van Nostrand, New York, 1953), Vol. 2.
- ²⁷Tosoh Corporation, 1-14-15 Akasaka, Minato-Ku, Tokyo 107, Japan.
- ²⁸Polymer Source, Inc. 771 Lajoie, Dorval, Quebec, Canada H9P 1G7.
- ²⁹J. François, F. Candau, and H. Benoit, *Polymer* **15**, 618 (1974).
- ³⁰F. Candau, J. François, and H. Benoit, *Polymer* **15**, 626 (1974).
- ³¹W. B. Li, P. N. Segre, R. W. Gammon, J. V. Sengers, and M. Lamvik, *J. Chem. Phys.* **101**, 5058 (1994).
- ³²W. Köhler (private communication).
- ³³T. G. Scholte, *J. Polym. Sci., Part A-2* **3**, 841 (1970).
- ³⁴R. Kniewske and W. Kulicke, *Makromol. Chem.* **184**, 2173 (1983).
- ³⁵B. Appelt and G. Meyerhoff, *Macromolecules* **13**, 657 (1980).
- ³⁶N. Nemoto, V. Makita, Y. Tsunashima, and M. Kurata, *Macromolecules* **17**, 425 (1984).
- ³⁷K. Huber, W. Burchard, and A. Z. Akcasu, *Macromolecules* **18**, 2743 (1985).
- ³⁸B. D. Freeman, D. S. Soane, and M. M. Denn, *Macromolecules* **23**, 245 (1990).
- ³⁹Y. Tsunashima, T. Hashimoto, and T. Nakano, *Macromolecules* **29**, 3475 (1996).
- ⁴⁰P. Rossmanith and W. Köhler, *Macromolecules* **29**, 3203 (1996).
- ⁴¹B. Nyström and J. Roots, *J. Polym. Sci., Part C: Polym. Lett.* **28**, 101 (1990).
- ⁴²B. Nyström and J. Roots, *Polymer* **33**, 1548 (1992).
- ⁴³Y. Shiwa, Y. Oono, and P. R. Baldwin, *Macromolecules* **21**, 208 (1988).
- ⁴⁴Y. Shiwa, *Phys. Rev. Lett.* **58**, 2102 (1987).
- ⁴⁵K. F. Freed, *J. Chem. Phys.* **79**, 6357 (1983).
- ⁴⁶B. J. Cherayil and K. F. Freed, *J. Chem. Phys.* **104**, 5983 (1996).
- ⁴⁷P. Wiltzius, H. R. Haller, D. S. Cannell, and D. W. Schaefer, *Phys. Rev. Lett.* **51**, 1183 (1983).